Embryonic Thermal Challenge is Associated with Increased Stressor Resiliency Later in Life: Molecular and Morphological Mechanisms in the Small Intestine

David L. Beck[1], Elizabeth R. Gilbert[1], Mark A. Cline[1]

[1]School of Neuroscience, Virginia Polytechnic Institute and State University, Blacksburg, VA, United States

Abstract

Developing chick embryos that are subjected to increased incubation temperature are more stressor-resilient later in life, but the underlying process is poorly understood. The potential mechanism may involve changes in small intestine function. In this study, we determined behavioral, morphological, and molecular effects of increased embryonic incubation temperatures and post-hatch heat challenge in order to understand how embryonic heat conditioning (EHC) affects gut function. At 4 days post-hatch, duodenum, jejunum, and ileum samples were collected at 0, 2, and 12 hours relative to the start of heat challenge. In EHC chicks, we found that markers of heat and oxidative stress were generally lower while those of nutrient transport and antioxidants were higher. Temporally, gene expression changes in response to the heat challenge were similar in control and EHC chicks for markers of heat and oxidative stress. Crypt depth was greater in control than EHC chicks at 2 hours post-challenge, and the villus height to crypt depth ratio increased from 2 to 12 hours in both control and EHC chicks. Collectively, these results suggest that EHC chicks might be more energetically efficient at coping with thermal challenge, preferentially allocating nutrients to other tissues while protecting the mucosal layer from oxidative damage. These results provide targets for future

studies aimed at understanding the molecular mechanisms underlying effects of embryonic heat exposure on intestinal function and stressor resiliency later in life.

Keywords

thermoregulation; antioxidant function; nutrient transport; intestinal morphology; oxidative damage

Declarations of interests: The authors declare that they have no known competing financial interests or personal relationships that could have appeared to influence the work reported in this paper.

Introduction

Heatwaves have been more frequent in recent years resulting in substantial animal fatalities and financial setbacks in the farming industry and poultry sector (Brugaletta et al., 2022). High environmental temperatures have the potential to affect living organisms through changes in metabolism, immune response, and cellular function (Dillon et al., 2010; Paital et al., 2016). Among the various organs affected, the small intestine is particularly prone to heat-related functional disruptions.

Physiological responses and long-term adaptations to high temperatures are relevant to both human and animal populations. One notable example is the leaky-gut hypothesis, which proposes that endotoxins, in poultry and humans alike, can translocate from the intestinal lumen into circulation from prolonged high internal body temperature (Rostagno, 2020; Garcia et al., 2022). Physiological ramifications include bacterial infections, systematic inflammation, and changes in microbiota composition (Mu et al., 2017; Rostagno, 2020). Heat stress and compromised gut function are associated with compromised health and well-being in animals such as swine (Mayorga et al., 2020). Growth, reproduction, and lactation are impaired due to reallocation of nutrients to survival-oriented behaviors and processes (Mayorga et al., 2020). These animal and agricultural implications can have profound impacts on welfare, costs of products, and availability of food.

Previous research pertaining to embryonic heat conditioning in broiler chicks showed that an elevation in incubation temperature can lead to increased stress resilience later in life (Rosenberg

et al., 2020). Depending on stressor intensity, embryonic heat manipulation can either promote vulnerability or resilience, and effects can be transgenerational (Rosenberg et al., 2022). Moreover, embryonic heat conditioning can increase heat and immunological cross-tolerance through epigenetic mechanisms such as hydroxymethylation (Rosenberg et al., 2020). This expands on the notion that in-utero environments impact the health and well-being of organisms later in life (Boekelheide et al., 2012). Prior embryonic heat conditioning research focused on the hypothalamus; thus, it remains unclear whether the effects of embryonic heat conditioning on the small intestine apply, persist, and promote a beneficial phenotype in times of heat stress. Thus, we determined effects of embryonic heat conditioning and early post-hatch heat challenge on behavior and small intestinal physiology in broiler chicks.

Materials and Methods

Animals

Cobb-500 broiler (*Gallus gallus*) eggs were obtained from a commercial hatchery. The eggs were randomly divided into incubation treatments of control (CTRL) and embryonic heat conditioned (EHC). CTRL eggs were incubated constantly at 37.5°C through the 21-day incubation period. From embryonic day 7 to 16, EHC eggs were incubated at 39.5°C from 19:30 to 07:30 and 37.5°C for the remainder of each day. From embryonic day 17 to 21, EHC eggs were incubated at an identical temperature to the CTRL group, 37.5°C. After hatch, chicks were raised in individual cages in climate-controlled rooms with temperatures at 31.5 ± 1°C and ad libitum access to feed and water. Diets were formulated to meet minimum recommended nutrient

levels for the starter phase of Cobb-500 chicks and formulations are published elsewhere. All trials were conducted at 4 days post-hatch. Experimental procedures were approved by the Virginia Tech Institutional Animal Care and Use Committee.

Experiments

Gene expression

On day 4 post-hatch, both CTRL and EHC chicks were divided into 3 groups (0, 2, and 12 hour) using a randomized complete block design, with body weight as the blocking factor, and chicks were thermally challenged by exposure to 36.7°C conditions for 12hrs. Feed and water were not withheld. Chicks were euthanized by decapitation and tissues were collected at 0 (before heat application), 2, and 12hrs relative to the start of the heat challenge. Sixty chicks (30 CTRL and 30 CTRL) were sampled for 1cm sections of the duodenum, jejunum, and ileum with ten samples from each group collected at each time-point. The duodenum sample was dissected at the distal portion of the duodenal loop. The jejunum was sampled midway between the end of the duodenal loop and Meckel's diverticulum (yolk sac remnant). The ileum was sampled midway between Meckel's diverticulum and the cecal tonsils. Samples were rinsed in ice-cold phosphate-buffered saline (PBS), blotted on a kimwipe, and submerged in RNAlater (Invitrogen, Waltham, MA), incubated at 4°C overnight, and then stored at -20°C until nucleic acid extraction.

Tissues of 10-20mg were homogenized in 1mL TRI Reagent (Molecular Research Center, Cincinnati, OH) using 5mm stainless steel beads (Qiagen, Germantown, MD) and a Tissue Lyser II (Qiagen) for 3 x 2min at 20Hz. After the step of adding equal parts 100% molecular biology-

grade ethanol, the lysate and ethanol mixture were transferred to spin columns and purified with RNase-free DNase I using the Direct-zol RNA miniprep kit (Zymo Research, Irvine, CA). Total RNA was quantified using an Implen NanoPhotometer at 260/280nm and stored at -80°C. Single-stranded cDNA was synthesized in 20µL reactions using the High-Capacity cDNA Archive Kit (Applied Biosystems, Waltham, MA) following the manufacturer's instructions: 25°C for 10 minutes, 37°C for 2 hours, and 85°C for 5 minutes. Primers were designed using Primer Express 3.0.1 (Applied Biosystems) (Table A.1). Real-time PCR was performed in 10µL reactions containing 5µL Fast SYBER Green Master Mix (Applied Biosystems), 0.25µL each of 5µM forward and reverse primers, 1.5µL of nuclease-free water, and 3µL of 10-fold diluted cDNA. Reactions were performed in duplicate using a 7500 FAST system (Applied Biosystems) and the default "FAST" program. Melting curve analyses were performed after PCR to ensure amplicon specificity.

Morphology

Samples of duodenum were rinsed in PBS and submerged in 10% neutral-buffered formalin, incubated on a rocker at 4°C overnight, and then rinsed in a graded ethanol series and stored in vials of 70% ethanol. The samples were shipped to StageBio (Mount Jackson, Virginia) for paraffin embedding and sectioning at 5µm with replicate sections collected at least 200 µm apart in the same tissue sample. Three to five cross-sections were prepared on each slide per sample, and slides were stained with hematoxylin and eosin. A Nikon Eclipse 80i microscope with Nikon DS-Ri2 color camera was used for brightfield microscopy and images were captured under a 2x objective. The Nikon Ni-S Elements AR 5.30.05 software (Nikon, Tokyo, Japan) was used to measure 10 villus heights and 10 crypt depths per chick. The villus was defined as the base

(before start of crypt) to the tip of the villus, and the crypt was defined as the base of the villus to the bottom of the invagination (Figure B.1).

Behavior and Food/Water Intake

At 4 days post-hatch, non-heat-challenged chicks were placed individually in a 290 x 290mm enclosed acrylic observation arena with food and water containers in diagonal corners. Food and water containers were massed before observation. Chicks were recorded from three angles for 30 minutes. Data were analyzed on a 300s basis using ANY-maze (Stoelting Co., Wood Dale, IL). Distance traveled (in meters), as well as the number of food pecks, water pecks, exploratory pecks, jumps, and escape attempts were quantified as count-type behaviors. Amount of time spent (s) standing, sitting, preening, perching, and sleeping were quantified as timed-type behaviors. Food/water pecks were defined as pecks within the food/water containers. Non-food/water-related pecks were counted as exploratory pecks. Sleeping was quantified starting after 3s of eye closure. After 30 minutes, the weights of the food and water containers were recorded. The difference between container weights was defined as food/water intake.

Statistical Analysis

Gene expression and morphology data were analyzed by analysis of variance (ANOVA) using JMP 17.2.0 (SAS Institute, Cary, NC) with Tukey's test used for post-hoc comparisons. The level of statistical significance for all analyses was set at $P \leq 0.05$. Gene expression data were analyzed using the DDC_T method (Schmittgen and Livak, 2008). Actin was used as the reference gene and the average of the duodenum of the CTRL group at time 0 served as the calibrator group. The first statistical model included the effect of EHC (CTRL vs. EHC), time-point (0hrs,

2hrs, 12hrs), and the two-way interaction, within an intestinal segment. The second model included all segments (duodenum, jejunum, ileum) and the three-way interaction between effect of EHC, time-point, and segment. For all analyses, sex was non-significant and thus removed from the model.

For morphological analyses, the statistical model included the effect of EHC, time-point, body weight, and the two-way interaction between effect of EHC and time-point. Body weights were analyzed by a T-test. A bivariate fit of body weight and corresponding morphological variables was used to determine correlation (r) and the linear model. Villus-height:crypt-depth (VCR) was calculated for each chick by dividing the corresponding average villus height by average crypt depth.

Behavioral data were analyzed by the Wilcoxon Rank Sum Test due to non-heterogenous variances. Food and water intake were analyzed by a T-test.

Sample sizes for each experiment are reported within corresponding tables.

Results

Gene Expression: mRNA Abundance

Tables A.2, A.3, A.4, and A.5 summarize results for mRNAs in the small intestine and then segmentally as the duodenum, jejunum, and ileum, respectively. A two-way interaction of treatment and time was observed for one gene (Figure B.2; described below).

Combined Segments

Treatment-wise, there were multiple main effects in the small intestine (Table A.2). There was greater expression of both heat shock protein 70 (HSP70) and heat shock protein 47 (HSP47) mRNAs in CTRL than EHC. Reactive oxygen species-related gene xanthene dehydrogenase (XDH) was also greater in CTRL than EHC. Superoxide dismutase 1 (SOD1) expression was greater in EHC than CTRL. Glucose transporter 2 (GLUT2) was greater in EHC than CTRL.

There were also several effects of time in the small intestine. HSP70 mRNA decreased from 2 to 12hrs during the heat challenge. XDH expression increased from 0 to 12hrs.

Segmentally, expression differed for almost every target gene. Hypoxia-inducible factor 1-alpha (HIF1A) was not affected. Glucose transporter 1 (GLUT1) expression increased from the duodenum to the ileum. GLUT2 expression was similar between the duodenum and jejunum and lower in the ileum than the prior two segments. Sodium-glucose cotransporter 1 (SGLT1) expression was highest in the duodenum with lower expression in the jejunum and ileum. HS47 expression decreased from the proximal to distal end of the small intestine. Heat shock protein 60 (HSP60) expression was similar in the duodenum and jejunum and lower in the ileum. HSP70 expression increased from the duodenum to jejunum and was similar to the duodenum in the

ileum. Heme oxygenase 2 (HMOX2) expression was highest in the duodenum with lower levels in the jejunum and ileum. Similarly, XDH expression was highest in the duodenum with lower levels in the jejunum and ileum. Glutathione peroxidase 7 (GPX7) expression decreased from the duodenum to the jejunum and then increased slightly to the ileum. SOD1 expression was similar in the duodenum and jejunum with lower expression in the ileum. Cytochrome c oxidase 16 (COX16) expression was highest in the duodenum and ileum with lower expression in the jejunum.

A treatment x time interaction was observed for XDH where there was an increase in CTRL mRNA from 0 to 12hrs (Figure B.2).

A treatment x segment interaction was observed for GLUT1 mRNA (Figure C.6). Segment x time interactions were observed for HSP70 (Figure C.7), HMOX2 (Figure C.8), and COX16 mRNA (figures included in supplemental figures).

Duodenum

There were several main effects of treatment in the duodenum (Table A.3). There was greater expression of HSP47 mRNA in CTRL than EHC. Reactive oxygen species-related genes HIF1A and XDH were also greater in CTRL than EHC.

There were also several effects of time in the duodenum. HSP70 expression increased in both groups from 0 to 2hrs and then returned to baseline by 12hrs. HSP47 expression was constant

from 0 to 2hrs and then decreased to 12hrs. HMOX2 increased from 0 to 2hrs in both CTRL and EHC with no difference from 2 to 12hrs.

Jejunum

In the jejunum (Table A.4), there was increased expression of GLUT2 mRNA in the EHC compared to CTRL group. SOD1 expression was higher in EHC compared to CTRL.

A main effect of time was observed for SGLT1 and XDH mRNAs. SGLT1 expression increased from 0 to 2hrs, while XDH expression increased from 2 to 12hrs.

Ileum

In the ileum (Table A.5), there were several treatment effects. GLUT1, GLUT2, and SGLT1 expression levels were higher in the EHC than CTRL group. HSP70 expression was greater in the CTRL group.

There were also a few effects of time in the ileum where GPX7 and COX16 mRNAs decreased from 0 to 2hrs. HSP70 and HMOX2 mRNA decreased from 0 to 12hrs.

Morphology

Histological analysis was focused on the duodenum. No treatment, time, or treatment x time differences were observed for villus height (Table A.6).

There was an interaction of treatment x time for crypt depth. Crypt depth increased between 0 and 2hrs in the CTRL group and remained constant in the EHC group.

The VCR increased from 2 to 12hrs.

Differences in body weight between groups was not statistically significant, with CTRL chicks having a mean weight at 87.67g and EHC chicks at 82.66g ($p = 0.31$). There was a significant linear relationship between morphological parameters and body weight; villus height and VCR increased as body weight increased (Figures B.4 and B.5, respectively).

Behavior

Behaviors were similar among groups. No differences were observed for food intake and water intake. CTRL chicks consumed $0.05g \pm 0.11$ of food and $0.19g \pm 0.27$ of water. EHC chicks consumed $0.28g \pm 0.11$ of food and $0.18g \pm 0.27$ of water. Other behaviors (Tables A.7, A.8) were similar except for time spent sitting at 2 time-points. The EHC group spent less time sitting than the CTRL at times 20 and 25min.

Discussion

Gene Expression

Heat shock proteins (HSP), which are distributed ubiquitously throughout the body, are crucial for maintaining cell health and integrity (Dudeja et al., 2009), and can be indicators of stress,

241 cytoprotection, and immune response activation (Liu et al., 2014). In our study, differences in
242 HSP mRNA were observed in the duodenum, ileum, and combined segments, with several
243 factors reduced in the EHC group independent of heat challenge. HSP70 is a factor that is
244 induced in response to thermal challenge and actively combats inflammation, apoptosis, and
245 protein misfolding (Kisliouk et al., 2017; Hao et al., 2018). HSP47 is also triggered during heat
246 exposure and serves to avert procollagen misfolding; however, its expression correlates directly
247 with collagen impairment, suggesting possible negative long-term impacts on growth (Siddiqui
248 et al., 2020).
249
250 Responses to heat stress can have profound impacts on aerobic metabolism, leading to heightened
251 oxidative stress across various tissues due to the generation of reactive oxygen species (Rhoads et
252 al., 2013). The production of reactive oxygen species can generate dysfunction in regulation of
253 gene expression and redox signaling, damage to proteins and DNA/RNA (Barboza et al., 2017),
254 as well as contribute to leaky gut syndrome through changes in the ratio of anti-inflammatory to
255 pro-inflammatory molecules and alterations in bacterial compositions (Shandilya et al., 2022). We
256 observed HIF1A, a hypoxia-inducible factor, to be greater in the CTRL group in the duodenum.
257 Hypoxia-inducible factors are activated during hypoxic conditions, which can be induced by
258 elevated ambient temperature, to regulate and adapt to a lack of oxygen delivery to internal organs
259 (Rhoads et al., 2013; Li et al., 2015). With HIF1A's role in regulating angiogenesis, it is apparent
260 that the EHC group may have programmed gene expression levels that alter how they react to
261 changes in oxygen levels, nutrient supply, or tissue damage (Marchesi et al., 2019). XDH
262 expression was also greater in the CTRL group in the duodenum, and in the jejunum, it increased
263 during the heat challenge in both groups. XDH activity can directly yield superoxide anions (Lee

et al., 2014), or post-translational modification can cause the conversion of XDH to XO (xanthine oxidase) and subsequent release of superoxide and hydrogen peroxide (Liang et al., 2024). XO's long half-life allows time for reactive oxygen species to diffuse into the bloodstream and create systematic effects (Liang et al., 2024).

Cellular antioxidant capacity is important to minimize oxidative stress. SOD, catalase, and GPX are enzymatic antioxidants that can react with potentially harmful substrates (Pei et al., 2023). SOD is responsible for the initial conversion of a superoxide anion into hydrogen peroxide whereas catalase and GPX reduce hydrogen peroxide into water and oxygen. We observed a higher expression of SOD1 in EHC chicks. SOD1 mRNA can be decreased due to heat stress (Belhadj Slimen et al., 2014) and elevated expression after EHC could suggest more optimal intestinal barrier integrity through an increase in growth of intestinal stem cells (Wang et al., 2022), and an overall greater capacity to reduce oxidative stress and thus restrict harmful inflammatory responses (Hwang et al., 2020).

Glucose, as a primary fuel source for cells throughout the body, is necessary for the production of ATP to support physiological processes (Nakrani et al., 2024). Glucose transporters are essential for nutrient uptake, metabolism, and sensing, which lead to the secretion of entero-hormones (Koepsell, 2020). While some of the differences were segment-specific, overall there were instances of greater GLUT1, GLUT2, and/or SGLT1 mRNA in EHC chicks. GLUT2 expression is down-regulated during heat stress (Sun et al., 2015; Al-Zghoul et al., 2019), and others showed that EHC leads to increases in intestinal SGLT1 expression (Rashid et al., 2016). In conjunction, SGLT1 and GLUT2 work to transport glucose from the lumen, into an enterocyte, and into a

capillary to eventually be available as an energy source. Since neither SGLT1 or GLUT2 expression levels were impacted by time during heat challenge, results suggest that EHC leads to greater metabolism of glucose or a preparation for rapid uptake of glucose to combat consequences of a stressor that may affect energy supply (Sun et al., 2023). As for GLUT1, hypoxic conditions can allow HIF1A to interact with HIF1B to increase GLUT1 expression, and oxidative stress caused by XO can directly upregulate GLUT1 expression (Liemburg-Apers et al., 2015). However, we saw no change of HIF1A or XDH mRNA abundance in EHC chicks. GLUT1, which is observed in most epithelial cells that border the vasculature (Koepsell, 2020), is typically more abundant in the colon than small intestine (Yoshikawa et al., 2011). Due to the young age of the chicks, GLUT1 expression in the ileum could be indicative of a still-developing organ (Aschenbach et al., 2009). GLUT1 can work as a compensatory mechanism in the large intestine to achieve greater blood glucose concentrations as it couples with SGLT1 in a similar fashion to GLUT2 (Yoshikawa et al., 2011). GLUT1 expression and circulating blood glucose are inversely correlated, and blood glucose typically increases with heat stress (Abbas et al., 2020). Thus, higher expression of GLUT1 in conjunction with higher expression of SGLT1 and GLUT2 in EHC chicks could indicate an adaptation to alleviate the physiological demands of hepatic or renal gluconeogenesis in response to heat stress (Watford, 1985; Kimball et al., 2018).

Morphology

Because of the pronounced temporal and treatment-related gene expression changes in the duodenum as well as its vital role in nutrient transport, absorption, and digestion, the duodenum was selected as the focus of the morphological analyses. Small intestinal morphological

parameters such as villus height, crypt depth, and VCR can indicate health of the small intestine and thus relative health of the organism. High temperatures alter small intestinal morphology by epithelial shedding and can increase crypt depth (Zhang et al., 2017; Ghulam Mohyuddin et al., 2022). In our study, villus height was not altered; however, crypts deepened in the CTRL group from 0 to 2hrs (Figure B.3). Crypt depth is a marker of nutrient digestion, nutrient absorption, and cell proliferation (Adeleye et al., 2018). The deepening of the crypt in the CTRL group could be indicative of a villus renewal process stimulated by inflammation by a stressor (Adeleye et al., 2018). Simultaneously, a deeper crypt would also suggest reduced digestion and absorption of nutrients, as it could suggest that more immature cells are being recruited to the villus that do not yet have complete nutrient digestive and absorptive functions (Blachier et al., 2022). Furthermore, the increase in VCR across the thermal challenge suggests higher rates of epithelial turnover and nutrient absorption (Marchewka et al., 2021). Body weight had some correlation to villus height and VCR but not crypt depth (Figures B.4, B.5).

Behavior

No difference was observed in food or water consumption between groups. Behaviorally, most count and time characteristics were similar. Given that sitting time (s) is not directly a stress-associated behavior and no other behaviors were affected, changes observed in the small intestine are likely not secondary to behavior modification.

Conclusion

Factors affected by EHC can be targeted for future studies aimed at understanding epigenetic changes that are likely occurring to cause these persistent gene expression effects. Although the

heat challenge did not accentuate or reveal changes that were EHC-specific, there were a number of gene expression differences that were identified independent of heat challenge. It is possible that our selection of sample times may have not captured the dynamics of the heat stress response, or it is possible that some of the changes occurred post-translationally. Measuring mRNA reflects a portion, albeit a large one, of how cellular activities are regulated and coordinated to maintain cellular integrity and adaptive responses to environmental stimuli. In conclusion, results suggest that EHC leads to gene expression differences in the small intestine that may reflect alterations in responses to oxidative stress and hence the ability to maintain barrier integrity and allocate sources of energy during a heat challenge.

Appendices

Appendix A

Table A.1. Primers used for real-time PCR

Gene[1]	Accession no.	Sequences (forward/reverse)
β-actin	NM_205518.2	GTCCACCGCAAATGCTTCTAA/TGCGCATTTATGGGTTTTGTT
GLUT1	NM_205209.2	TCCTGATCAACCGCAATGAG/TGCCCCGGAGCTTCTTG
GLUT2	NM_207178	GAAGGTGGAGGAGGCCAAA/TTTCATCGGGTCACAGTTTCC
SGLT1	XM_046928028.1	GCCTCGAGCAGATTCTTTTCA/CCCTGGCCATGGCAGAT
HSP47	XM_046906875.1	TCATGGTGACCCGCTCCTA/TGTAGAGACCTGTACGATGCATCA
HSP60	NM_001012916.3	CGCAGACATGCTCCGTTTG/TCTGGACACCGGCCTGAT
HSP70	NM_001006685.2	TCGGCCGCAAGTATGATGA/CGGAAGGGCCAGTGCTT
HMOX2	XM_040684169.2	GTGGAGTTGACTGCAGGGAAA/TGGATAGTCCCCCTGGATTTT
HIF1A	XM_040700545.2	TGGCAATGTCCCCACTACCT/GGATCGGCATTGCTACGAA
XDH	XM_046913190.1	GGCATTCTCTAGGGTCAGTCTCTT/CAAAACTAAGGGTTGTCTTGAAAAGG
GPX7	NM_001163245.2	TCTAGCCATGCTCCTTGCAA/TGCTGAGTAGCGGAAAATGCT
SOD1	NM_205064.2	TGGCTTCCATGTGCATGAAT/AGCACCTGCGCTGGTACAC
COX16	XM_046918459.1	TGATGCAGCTATACCAACGCTTA/

		TTCATGTGCAAGTCTGCCTAGTG

[1] Primers for β-actin (Actin), glucose transporter 1 (GLUT1), glucose transporter 2 (GLUT2), sodium-glucose cotransporter 1 (SGLT1), heat shock protein 47 (HSP47), heat shock protein 60 (HSP60), heat shock protein 70 (HSP70), heme oxygenase 2 (HMOX2), hypoxia-inducible factor 1-alpha (HIF1A), xanthene dehydrogenase (XDH), glutathione peroxidase 7 (GPX7) cytochrome c oxidase 16 (COX16), and superoxide dismutase 1 (SOD1).

Table A.2 Fold difference in mRNA of target genes[1] in the small intestine (duodenum, jejunum, ileum) of 4-day old chickens.

Small Intestine[2]	GLUT1	GLUT2	SGLT1	HSP47	HSP60	HSP70
Treatment[3]						
CTRL	1.22±0.06	0.72±0.06	0.50±0.04	0.81±0.03	0.80±0.04	1.54±0.10
EHC	1.32±0.06	0.95±0.06	0.56±0.04	0.72±0.03	0.83±0.04	1.17±0.10
P-value	0.185	**0.008**	0.220	**0.047**	0.721	**0.011**
Time						
0	1.30±0.07	0.90±0.07	0.50±0.04	0.80±0.04	0.88±0.05	1.46^{a}±0.12
2	1.25±0.07	0.81±0.07	0.60±0.04	0.81±0.04	0.88±0.05	1.58^{a}±0.12
12	1.25±0.07	0.78±0.07	0.48±0.04	0.68±0.04	0.70±0.05	1.04^{b}±0.12
P-value	0.846	0.498	0.122	**0.043**	0.0503	**0.006**
Segment						
Duodenum	1.08^{b}±0.07	0.96^{a}±0.07	1.09^{a}±0.04	0.93^{a}±0.04	1.01^{a}±0.05	1.36^{b}±0.12
Jejunum	1.30^{ab}±0.07	1.15^{a}±0.07	0.25^{b}±0.04	0.78^{b}±0.04	1.11^{a}±0.05	1.75^{a}±0.12
Ileum	1.42^{a}±0.07	0.39^{b}±0.07	0.26^{b}±0.04	0.59^{c}±0.04	0.33^{b}±0.05	0.97^{b}±0.12
P-value	**0.0027**	**<0.0001**	**<0.0001**	**<0.0001**	**<0.0001**	**0.0001**
Treatment x Time	0.984	0.893	0.661	0.889	0.946	0.623
Treatment x Segment	**0.047**	0.177	0.776	0.139	0.955	0.268
Segment x Time	0.463	0.404	0.354	0.092	0.243	**0.010**
Treatment x Time x Segment	0.793	0.699	0.980	0.988	0.886	0.159

Table A.2.1

Small Intestine[2]	HMOX2	HIF1A	XDH	GPX7	SOD1	COX16
Treatment[3]						
CTRL	1.01±0.07	1.04±0.05	1.05±0.05	0.58±0.04	0.85±0.04	1.00±0.14
EHC	0.96±0.07	0.96±0.05	0.90±0.05	0.56±0.04	0.97±0.04	0.84±0.14
P-value	0.689	0.245	**0.035**	0.744	**0.044**	0.423
Time						
0	0.89±0.09	0.91±0.06	0.85^{b}±0.06	0.64±0.05	0.87±0.05	0.98±0.18
2	1.13±0.09	1.09±0.06	0.97^{ab}±0.06	0.59±0.05	0.93±0.05	0.96±0.18
12	0.93±0.09	0.99±0.05	1.10^{a}±0.06	0.49±0.05	0.93±0.05	0.82±0.17
P-value	0.151	0.105	**0.014**	0.093	0.643	0.776
Segment						
Duodenum	1.54^{a}±0.09	1.10±0.06	1.29^{a}±0.06	0.83^{a}±0.05	1.09^{a}±0.05	1.29^{a}±0.18
Jejunum	0.62^{b}±0.09	0.99±0.06	0.83^{b}±0.06	0.35^{c}±0.05	1.16^{a}±0.05	0.49^{b}±0.18
Ileum	0.80^{b}±0.09	0.91±0.06	0.81^{b}±0.06	0.53^{b}±0.05	0.48^{b}±0.05	0.98^{ab}±0.18
P-value	**<0.0001**	0.078	**<0.0001**	**<0.0001**	**<0.0001**	**0.007**
Treatment x Time	0.671	0.339	**0.043**	0.393	0.427	0.865
Treatment x Segment	0.482	0.057	0.199	0.292	0.097	0.139
Segment x Time	**0.0002**	0.858	0.166	0.146	0.968	**0.003**
Treatment x Time x Segment	0.986	0.668	0.687	0.455	0.861	0.969

[1]GLUT 1,2 = glucose transporter 1 and 2; HSP47, 60, 70 = heat shock protein 47, 60, and 70; HMOX2 = heme oxygenase 2; HIF1A = hypoxia inducible factor 1-alpha; XDH = xanthene dehydrogenase; GPX7 = glutathione peroxidase 7; COX16 = cytochrome c oxidase 16.

[2] Values represent least square means ± SEM (n = 5-8 per treatment, per time, per segment), and *P*-values for main effects of treatment, time, and segment, and the corresponding two-way and three-way interaction(s) in the small intestine. Data were analyzed

using the $\Delta\Delta C_T$ method and relative quantity values were used for statistical analysis. Values without a common superscript within a row and effect differ ($P \leq 0.05$).

[3] CTRL = control; EHC = embryonic heat conditioned chicks.

Table A.3 Fold difference in mRNA of target genes[1] in the duodenum in 4-day old chickens.

Duodenum[2]	GLUT1	GLUT2	SGLT1	HSP47	HSP60	HSP70
Treatment[3]						
CTRL	1.14±0.09	0.92±0.09	1.03±0.10	1.04±0.07	1.01±0.09	1.53±0.15
EHC	1.02±0.09	0.99±0.09	1.14±0.10	0.82±0.07	1.01±0.09	1.18±0.15
P-value	0.321	0.554	0.472	**0.027**	0.992	0.105
Time						
0	1.03±0.11	1.14±0.11	1.07±0.12	1.00^{ab}±0.09	1.10±0.12	1.20^{b}±0.18
2	1.19±0.11	0.99±0.11	1.24±0.12	1.04^{a}±0.09	1.16±0.12	1.88^{a}±0.18
12	1.03±0.11	0.75±0.11	0.94±0.12	0.75^{b}±0.09	0.76±0.12	0.99^{b}±0.18
P-value	0.467	0.059	0.244	**0.043**	0.051	**0.003**
Treatment x Time	0.732	0.824	0.884	0.848	0.848	0.336

Table A.3.1

Duodenum[2]	HMOX2	HIF1A	XDH	GPX7	SOD1	COX16
Treatment[3]						
CTRL	1.64±0.19	1.26±0.10	1.45±0.09	0.90±0.10	1.10±0.09	1.65±0.39
EHC	1.43±0.19	0.93±0.10	1.12±0.09	0.77±0.10	1.08±0.09	0.93±0.39
P-value	0.435	**0.034**	**0.012**	0.346	0.870	0.203
Time						
0	1.02$^{\mathbf{b}}$±0.23	0.96±0.12	1.09±0.11	0.78±0.12	1.05±0.11	0.68±0.48
2	2.11$^{\mathbf{a}}$±0.23	1.23±0.12	1.35±0.11	0.96±0.12	1.13±0.11	1.68±0.48
12	1.48$^{\mathbf{ab}}$±0.23	1.11±0.12	1.41±0.10	0.76±0.12	1.09±0.12	1.51±0.47
P-value	**0.010**	0.305	0.090	0.453	0.889	0.298
Treatment x Time	0.874	0.605	0.124	0.341	0.970	0.881

[1] GLUT 1,2 = glucose transporter 1 and 2; HSP47, 60, 70 = heat shock protein 47, 60, and 70; HMOX2 = heme oxygenase 2; HIF1A = hypoxia inducible factor 1-alpha; XDH = xanthene dehydrogenase; GPX7 = glutathione peroxidase 7; COX16 = cytochrome c oxidase 16.

[2] Values represent least square means ± SEM (n = 6-8 per treatment, per time), and *P*-values for main effects of treatment, time, and the treatment by time interaction in the duodenum. Data were analyzed using the $\Delta\Delta C_T$ method and relative quantity values were used for statistical analysis. Values without a common superscript within a row and effect differ ($P \leq 0.05$).

[3] CTRL = control; EHC = embryonic heat conditioned chicks.

Table A.4 Fold difference in mRNA of target genes[1] in the jejunum in 4-day old chickens.

Jejunum[2]	GLUT1	GLUT2	SGLT1	HSP47	HSP60	HSP70
Treatment[3]						
CTRL	1.26±0.09	0.92±0.15	0.24±0.02	0.80±0.05	1.09±0.08	1.80±0.13
EHC	1.34±0.08	1.37±0.15	0.26±0.02	0.75±0.05	1.14±0.08	1.70±0.13
P-value	0.531	**0.037**	0.524	0.576	0.705	0.613
Time						
0	1.36±0.10	1.17±0.18	0.20^{b}±0.02	0.73±0.06	1.22±0.10	1.64±0.16
2	1.17±0.11	1.06±0.19	0.29^{a}±0.02	0.80±0.06	1.09±0.11	2.07±0.17
12	1.38±0.10	1.20±0.18	0.25^{ab}±0.02	0.80±0.06	1.03±0.10	1.55±0.16
P-value	0.317	0.857	**0.034**	0.601	0.482	0.071
Treatment x Time	0.610	0.755	0.403	0.998	0.827	0.808

Table A.4.1

Jejunum[2]	HMOX2	HIF1A	XDH	GPX7	SOD1	COX16
Treatment[3]						
CTRL	0.59±0.04	0.96±0.07	0.88±0.09	0.36±0.04	1.01±0.08	0.51±0.07
EHC	0.65±0.04	1.01±0.07	0.78±0.08	0.34±0.04	1.31±0.08	0.47±0.07
P-value	0.260	0.627	0.433	0.679	**0.012**	0.729
Time						
0	0.66±0.04	0.93±0.09	0.76^{ab}±0.10	0.40±0.05	1.13±0.10	0.46±0.09
2	0.56±0.05	1.02±0.09	0.66^{b}±0.11	0.36±0.05	1.14±0.10	0.52±0.09
12	0.64±0.04	1.00±0.09	1.07^{a}±0.10	0.28±0.05	1.22±0.10	0.48±0.08
P-value	0.266	0.777	**0.022**	0.168	0.807	0.920
Treatment x Time	0.883	0.232	0.729	0.504	0.324	0.409

[1] GLUT 1,2 = glucose transporter 1 and 2; HSP47, 60, 70 = heat shock protein 47, 60, and 70; HMOX2 = heme oxygenase 2; HIF1A = hypoxia inducible factor 1-alpha; XDH = xanthene dehydrogenase; GPX7 = glutathione peroxidase 7; COX16 = cytochrome c oxidase 16.

[2] Values represent least square means ± SEM (n = 5-8 per treatment, per time), and *P*-values for main effects of treatment, time, and the treatment by time interaction in the jejunum. Data were analyzed using the $\Delta\Delta C_T$ method and relative quantity values were used for statistical analysis. Values without a common superscript within a row and effect differ ($P \leq 0.05$).

[3] CTRL = control; EHC = embryonic heat conditioned chicks.

Table A.5 Fold difference in mRNA of target genes[1] in the ileum in 4-day old chickens.

Ileum[2]	GLUT1	GLUT2	SGLT1	HSP47	HSP60	HSP70
Treatment[3]						
CTRL	1.24±0.12	0.31±0.05	0.22±0.02	0.60±0.05	0.32±0.03	1.30±0.22
EHC	1.61±0.13	0.47±0.05	0.29±0.02	0.59±0.05	0.34±0.03	0.64±0.24
P-value	**0.040**	**0.049**	**0.034**	0.799	0.641	**0.047**
Time						
0	1.52±0.15	0.39±0.07	0.23±0.03	0.69±0.06	0.33±0.04	1.55^{a}±0.28
2	1.40±0.16	0.38±0.06	0.28±0.03	0.60±0.06	0.33±0.03	0.78^{ab}±0.28
12	1.35±0.15	0.40±0.06	0.25±0.03	0.50±0.06	0.31±0.03	0.58^{b}±0.28
P-value	0.719	0.979	0.493	0.094	0.929	**0.046**
Treatment x Time	0.850	0.183	0.179	0.952	0.425	0.201

Table A.5.1

Ileum[2]	HMOX2	HIF1A	XDH	GPX7	SOD1	COX16
Treatment[3]						
CTRL	0.78±0.08	0.90±0.07	0.82±0.08	0.49±0.07	0.43±0.04	0.85±0.16
EHC	0.82±0.08	0.92±0.08	0.79±0.09	0.58±0.07	0.52±0.04	1.11±0.16
P-value	0.768	0.823	0.811	0.323	0.101	0.273
Time						
0	1.01^{a}±0.10	0.84±0.09	0.70±0.11	0.74^{a}±0.08	0.42±0.05	1.80^{a}±0.20
2	0.72^{ab}±0.10	1.03±0.09	0.90±0.11	0.45^{b}±0.08	0.52±0.05	0.67^{b}±0.20
12	0.68^{b}±0.10	0.86±0.09	0.82±0.10	0.42^{b}±0.08	0.49±0.05	0.46^{b}±0.21
P-value	**0.037**	0.283	0.423	**0.018**	0.370	**<0.0001**
Treatment x Time	0.531	0.575	0.194	0.511	0.808	0.959

[1] GLUT 1,2 = glucose transporter 1 and 2; HSP47, 60, 70 = heat shock protein 47, 60, and 70; HMOX2 = heme oxygenase 2; HIF1A = hypoxia inducible factor 1-alpha; XDH = xanthene dehydrogenase; GPX7 = glutathione peroxidase 7; COX16 = cytochrome c oxidase 16.

[2] Values represent least square means ± SEM (n = 6-8 per treatment, per time), and *P*-values for main effects of treatment, time, and the treatment by time interaction in the ileum. Data were analyzed using the $\Delta\Delta C_T$ method and relative quantity values were used for statistical analysis. Values without a common superscript within a row and effect differ ($P \leq 0.05$).

[3] CTRL = control; EHC = embryonic heat conditioned chicks.

Table A.6 Duodenal villus height, crypt depth, and villus-height:crypt-depth in 4-day old chicks[1].

	Villus Height (µm) [2]	Crypt Depth (µm) [2]	Villus-height:Crypt-depth[2]
Treatment[3]			
CTRL	894.68±25.52	202.32±3.91	4.48±0.15
EHC	881.41±25.67	188.54±3.91	4.64±0.14
P-value	0.711	**0.018**	0.432
Time			
0	855.73±30.97	183.34^{b}±4.74	4.69^{ab}±0.18
2	893.59±32.48	213.62^{a}±5.20	4.14^{b}±0.19
12	914.81±28.67	189.33^{b}±4.39	4.85^{a}±0.16
P-value	0.382	**0.0004**	**0.021**
Treatment x Time	0.532	**0.025**	0.115
Body Weight	**0.0005**	0.566	**0.028**

[1] Values represent least square means ± SEM from 10 measurements of villus height and 10 measurements of crypt depth per chick (n = 5-7; per treatment per time-point), and *P*-values for main effects of treatment, time, the treatment by time interaction, and correlation to body weight ("Body Weight") in the duodenum. Values without a common superscript within a row and effect differ ($P \leq 0.05$).

[2] The villus height was defined as the top of the crypt to the tip of the villus, and the crypt depth was defined as the bottom of the villus to the bottom of the invagination beside the crypt. Villus-height:crypt-depth is the ratio of villus height to crypt depth.

[3] CTRL = control; EHC = embryonic heat conditioned chicks.

Table A.7 Count-type behaviors in chicks (Experiment 3)[1].

* Significantly different ($P \leq 0.05$) from CTRL.

		Time (min)					
Behavior	Treatment[2]	5	10	15	20	25	30
Steps (n)	CTRL	31.6 ± 9.7	50.3 ± 13.5	73.5 ± 21.9	84.9 ± 23.1	99.0 ± 25.3	112.6 ± 31.6
	EHC	30.50 ± 7.28	61.20 ± 13.19	87.0 ± 21.2	107.6 ± 26.7	121.5 ± 31.9	127.8 ± 34.5
Distance Traveled (m)	CTRL	1.9 ± 0.5	3.0 ± 0.7	4.5 ± 1.2	5.5 ± 1.3	6.4 ± 1.5	7.5 ± 1.9
	EHC	2.3 ± 0.4	4.1 ± 0.7	5.7 ± 1.1	7.6 ± 1.7	8.6 ± 2.2	9.0 ± 2.4
Water Pecks (n)	CTRL	0.0	0.0	0.0	0.0	0.0	0.0
	EHC	0.0	0.07 ± 0.07	0.15 ± 0.10	0.4 ± 0.2	0.4 ± 0.2	0.6 ± 0.3
Food Pecks (n)	CTRL	20.1 ± 12.19	38.1 ± 27.6	45.9 ± 34.8	65.3 ± 37.2	68.7 ± 37.0	68.9 ± 37.0
	EHC	0.54 ± 0.27	0.77 ± 0.32	1.23 ± 0.60	1.38 ± 0.62	1.62 ± 0.73	14.0 ± 8.83
Jumps (n)	CTRL	0.0	0.0	0.27 ± 0.27	0.55 ± 0.45	0.64 ± 0.54	0.73 ± 0.63
	EHC	0.07 ± 0.07	0.15 ± 0.1	0.23 ± 0.16	0.23 ± 0.17	0.23 ± 0.17	0.23 ± 0.17
Escape Attempts (n)	CTRL	0.54 ± 0.25	0.64 ± 0.31	0.72 ± 0.38	0.82 ± 0.38	0.82 ± 0.38	0.91 ± 0.46
	EHC	0.15 ± 0.10	0.23 ± 0.12	0.54 ± 0.27	0.77 ± 0.34	0.85 ± 0.34	0.92 ± 0.34

[1] Values are the means ± SEM. Data are from 11-13 chicks per treatment.

[2] CTRL = control; EHC = embryonic heat conditioned chicks.

462 **Table A.8** Timed-type behaviors in chicks (Experiment 3)[1].

463 * Significantly different ($P \leq 0.05$) from CTRL.

		Time (min)					
Behavior	Treatment[2]	5	10	15	20	25	30
Preening Time (sec)	CTRL	0.99 ± 0.68	1.40 ± 0.97	1.40 ± 0.97	1.51 ± 0.97	3.92 ± 1.73	3.92 ± 1.73
	EHC	0.70 ± 0.51	0.82 ± 0.51	0.82 ± 0.51	1.40 ± 0.71	1.80 ± 1.04	1.80 ± 1.04
Standing Time (sec)	CTRL	241.6 ± 27.6	433. 6 ± 63.1	568 ± 97.1	694.8 ± 130.9	823.5 ± 166.2	929.0 ± 203.9
	EHC	250.2 ± 19.9	480.5 ± 36.9	666.8 ± 62.9	847.2 ± 98.1	996.2 ± 134.1	1125.0 ± 166.3
Sitting Time (sec)	CTRL	42.8 ± 23.1	81.9 ± 29.6	145.9 ± 39.4	181.6 ± 43.8	195.7 ± 46.6	203.8 ± 48.0
	EHC	25.7 ± 18.4	28.8 ± 25.0	61.5 ± 29.4	79.4 ± 41.4*	81.8 ± 42.8*	111.8 ± 54.0
Perching Time (sec)	CTRL	11.9 ± 7.8	12.6 ± 7.9	14.6 ± 7.8	24.8 ± 10.3	27.8 ± 10.4	27.8 ± 10.4
	EHC	8.3 ± 8.2	15.7 ± 14.3	18.4 ± 14.5	22.1 ± 18.1	23.3 ± 17.9	47.79 ± 28.5
Sleeping Time (sec)	CTRL	0.0	67.5 ± 35.3	166.4 ± 75.4	282.4 ± 108.9	432.6 ± 146.0	611.2 ± 180.8
	EHC	12.1 ± 9.8	39.2 ± 24.8	136.8 ± 51.9	234.3 ± 85.6	381.3 ± 119.1	498.4 ± 149.9

464 [1] Values are the means ± SEM. Data are from 11-13 chicks per treatment.

465 [2] CTRL = control; EHC = embryonic heat conditioned chicks.

Appendix B

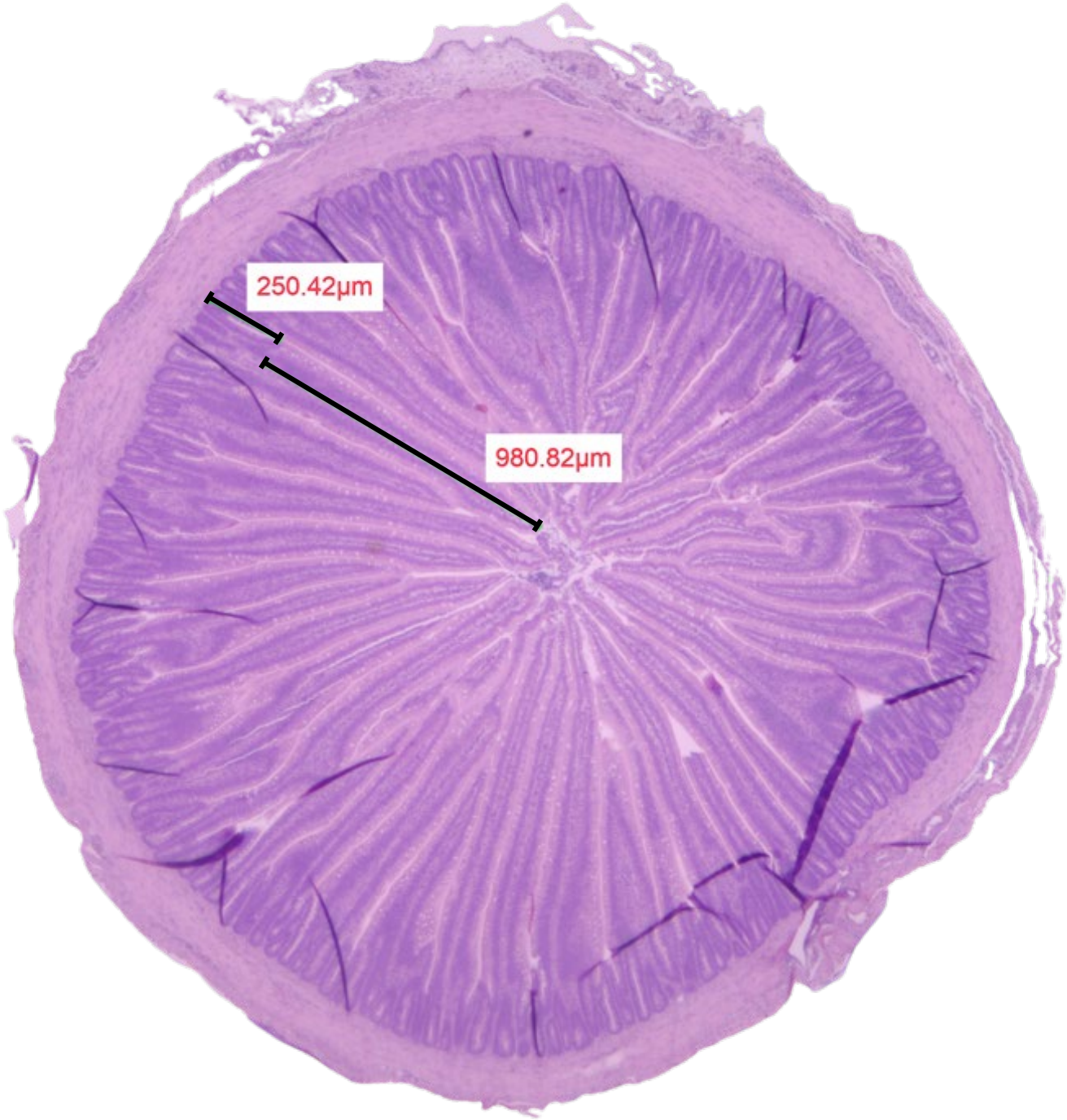

Fig. B.1. Representative cross-section from EHC chick with example measurements of villus height and crypt depth. 980.82 micrometers

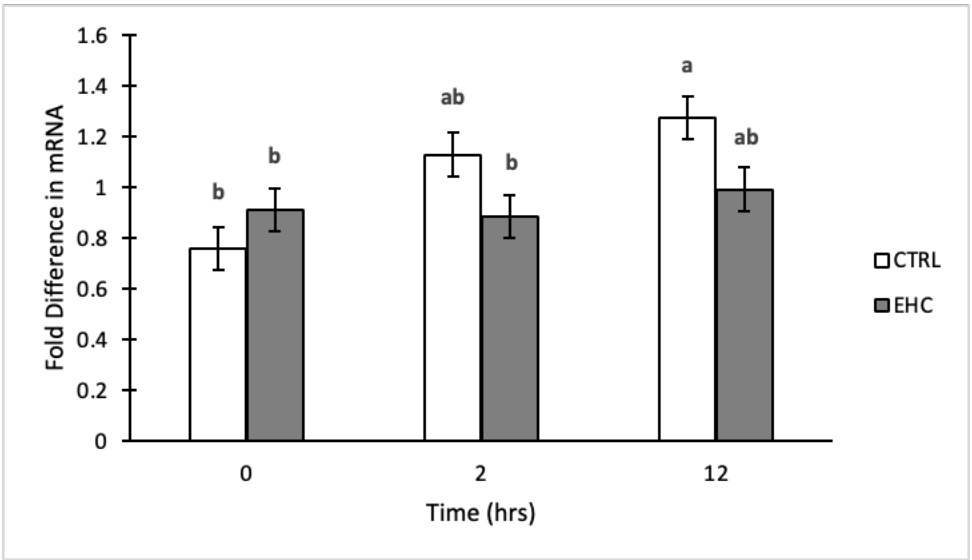

Fig. B.2. XDH (xanthene dehydrogenase) mRNA in the small intestine. XDH increased in the CTRL (control) group between time 0 and time 12. No differences were observed in the EHC (embryonic heat conditioned) group. Times (0, 2, 12) represent duration of exposure to a heat challenge. Values are least squares means ± SEM. Bars with unique superscripts are different ($P \leq 0.05$).

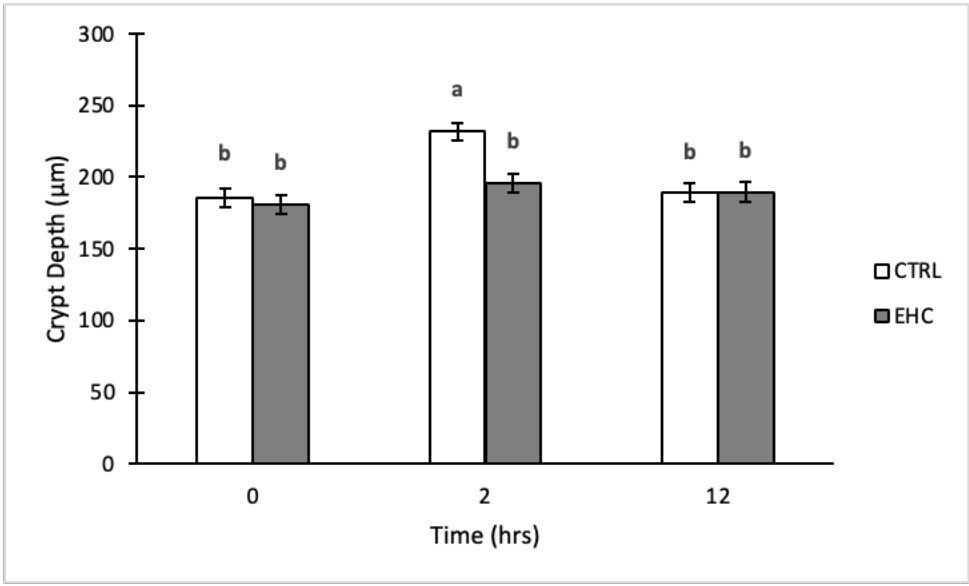

Fig. B.3. Crypt depth (µm) in duodenum over time (0, 2, 12hrs) in 4-day old chicks. An increase in crypt depth occurred between 0 and 2hrs for CTRL with a return to baseline by 12hrs. Times (0, 2, 12) represent duration of exposure to a heat challenge. Values are least squares means ± SEM. Bars with unique superscripts are different ($P \leq 0.05$).

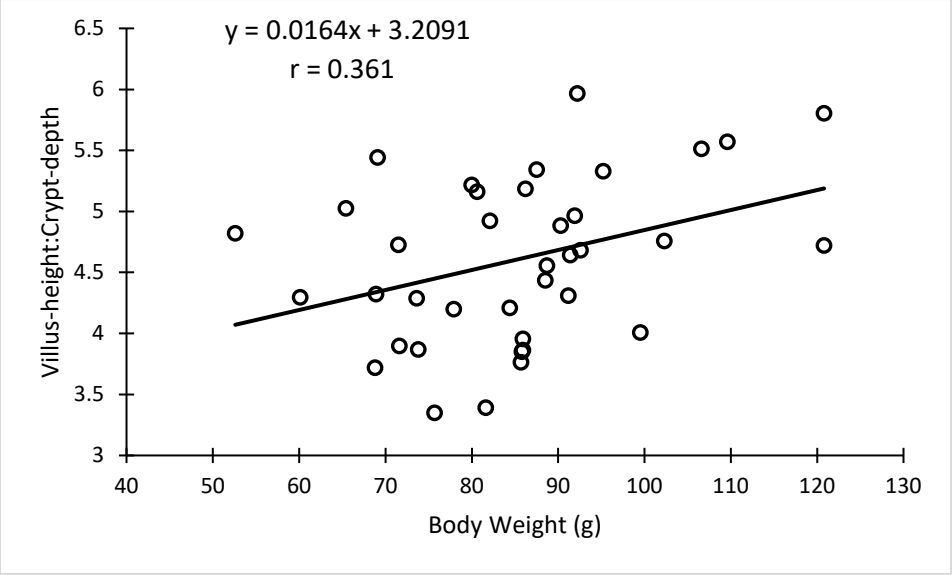

Fig. B.4. Scatterplot of relationship between body weight (g) and villus-height to crypt-depth ratio in 4-day old chicks.

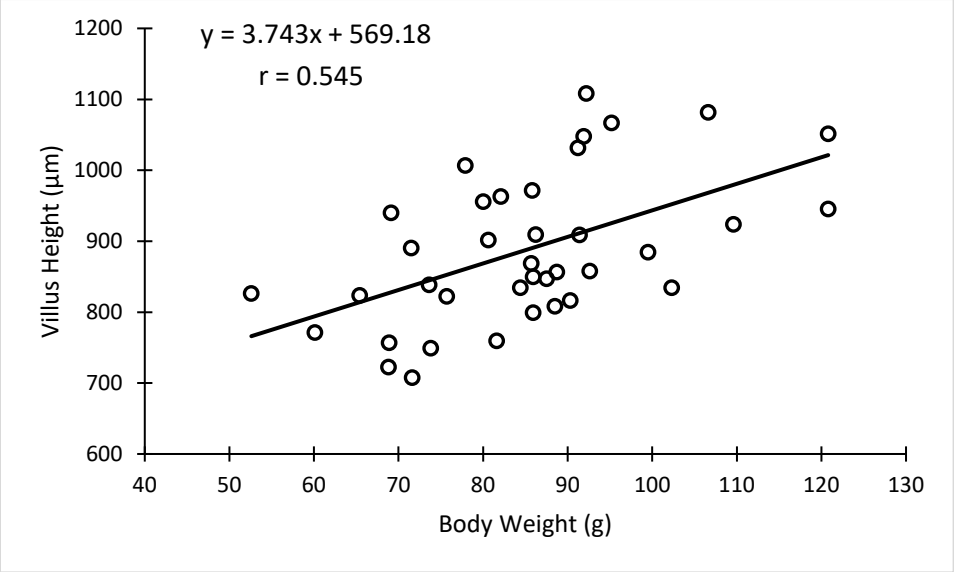

Fig. B.5. Scatterplot showing relationship between body weight (g) and villus height (µm) in 4-day old chicks.

Appendix C (Supplemental Figures)

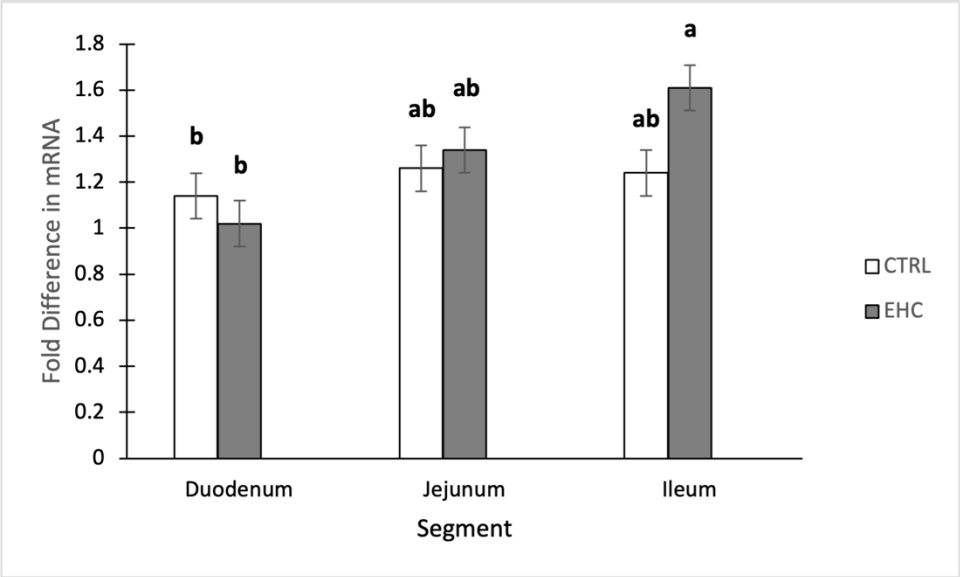

Fig. C.6. GLUT1 (glucose transporter 1) mRNA expression in the combined segments. Values are least squares means ± SEM. Bars with unique superscripts are different ($P \leq 0.05$).

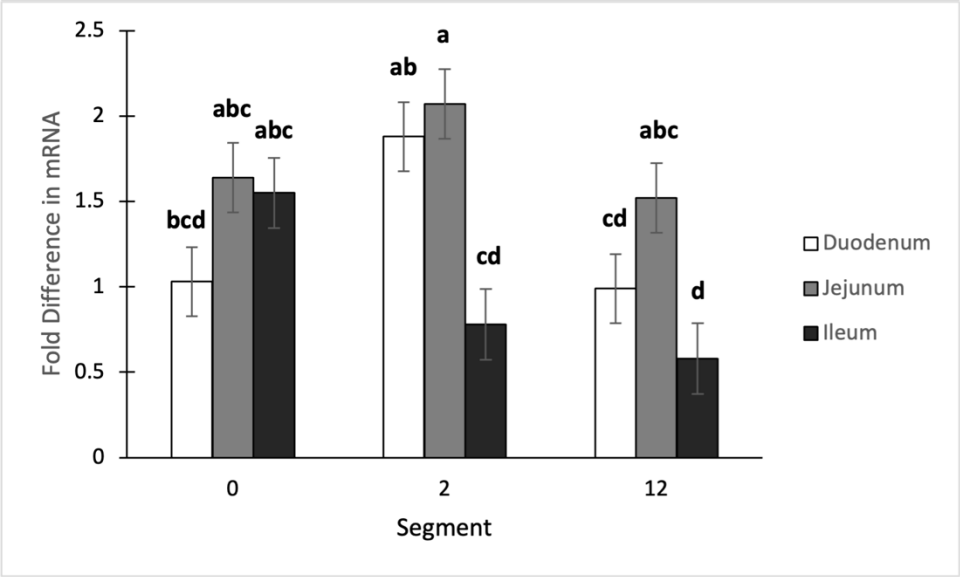

570

571 **Fig. C.7.** HSP70 (heat shock protein 70) mRNA expression in the combined segments. Values

572 are least squares means ± SEM. Bars with unique superscripts are different ($P \leq 0.05$).

573

574
575
576
577
578
579
580
581
582
583
584
585
586
587

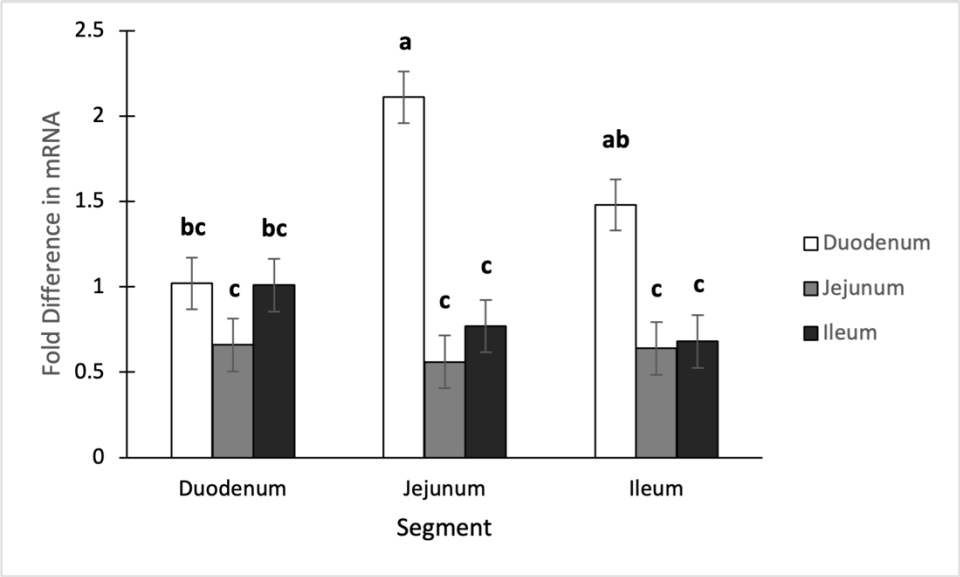

588

589 **Fig. C.8.** HMOX2 (heme oxygenase 2) mRNA expression in the combined segments. Values are

590 least squares means ± SEM. Bars with unique superscripts are different ($P \leq 0.05$).

591
592
593
594
595
596
597
598
599
600
601
602
603
604

References

Abbas, Z., Sammad, A., Hu, L., Fang, H., Xu, Q., Wang, Y., 2020. Glucose Metabolism and Dynamics of Facilitative Glucose Transporters (GLUTs) under the Influence of Heat Stress in Dairy Cattle. Metabolites 10, 312. https://doi.org/10.3390/metabo10080312

Adeleye, O.O., Otakoya, I.O., Fafiolu, A.O., Alabi, J.O., Egbeyale, L.T., Idowu, O.M.O., 2018. Serum chemistry and gut morphology of two strains of broiler chickens to varying interval of post hatch feeding. Veterinary and Animal Science 5, 20–25. https://doi.org/10.1016/j.vas.2017.12.001

Al-Zghoul, M., Alliftawi, A., Saleh, K., Jaradat, Z., 2019. Expression of digestive enzyme and intestinal transporter genes during chronic heat stress in the thermally manipulated broiler chicken. Poultry Science 98. https://doi.org/10.3382/ps/pez249

Aschenbach, J.R., Steglich, K., Gäbel, G., Honscha, K.U., 2009. Expression of mRNA for glucose transport proteins in jejunum, liver, kidney and skeletal muscle of pigs. J Physiol Biochem 65, 251–266. https://doi.org/10.1007/BF03180578

Barboza, G.D. de, Guizzardi, S., Moine, L., Talamoni, N.T. de, 2017. Oxidative stress, antioxidants and intestinal calcium absorption. World Journal of Gastroenterology 23, 2841–2853. https://doi.org/10.3748/wjg.v23.i16.2841

Belhadj Slimen, I., Najar, T., Ghram, A., Dabbebi, H., Ben Mrad, M., Abdrabbah, M., 2014. Reactive oxygen species, heat stress and oxidative-induced mitochondrial damage. A review. International Journal of Hyperthermia 30, 513–523. https://doi.org/10.3109/02656736.2014.971446

Blachier, F., Andriamihaja, M., Kong, X.-F., 2022. Fate of undigested proteins in the pig large intestine: What impact on the colon epithelium? Animal Nutrition 9, 110–118. https://doi.org/10.1016/j.aninu.2021.08.001

Boekelheide, K., Blumberg, B., Chapin, R.E., Cote, I., Graziano, J.H., Janesick, A., Lane, R., Lillycrop, K., Myatt, L., States, J.C., Thayer, K.A., Waalkes, M.P., Rogers, J.M., 2012. Predicting Later-Life Outcomes of Early-Life Exposures. Environ Health Perspect 120, 1353–1361. https://doi.org/10.1289/ehp.1204934

Brugaletta, G., Teyssier, J.-R., Rochell, S.J., Dridi, S., Sirri, F., 2022. A review of heat stress in chickens. Part I: Insights into physiology and gut health. Front Physiol 13, 934381. https://doi.org/10.3389/fphys.2022.934381

Dillon, M.E., Wang, G., Huey, R.B., 2010. Global metabolic impacts of recent climate warming. Nature 467, 704–706. https://doi.org/10.1038/nature09407

Dudeja, V., Vickers, S.M., Saluja, A.K., 2009. The role of heat shock proteins in gastrointestinal diseases. Gut 58, 1000–1009. https://doi.org/10.1136/gut.2007.140194

Garcia, C.K., Renteria, L.I., Leite-Santos, G., Leon, L.R., Laitano, O., 2022. Exertional heat stroke: pathophysiology and risk factors. BMJ Med 1, e000239. https://doi.org/10.1136/bmjmed-2022-000239

Ghulam Mohyuddin, S., Khan, I., Zada, A., Qamar, A., Arbab, A.A.I., Ma, X., Yu, Z., Liu, X.-X., Yong, Y.-H., Ju, X.H., Zhang-Ping, Y., Yong Jiang, M., 2022. Influence of Heat Stress on Intestinal Epithelial Barrier Function, Tight Junction Protein, and Immune and Reproductive Physiology. Biomed Res Int 2022, 8547379. https://doi.org/10.1155/2022/8547379

Hao, Y., Feng, Y., Li, J., Gu, X., 2018. Role of MAPKs in HSP70's Protection against Heat Stress-Induced Injury in Rat Small Intestine. Biomed Res Int 2018, 1571406. https://doi.org/10.1155/2018/1571406

Hwang, J., Jin, J., Jeon, S., Moon, S.H., Park, M.Y., Yum, D.-Y., Kim, J.H., Kang, J.-E., Park, M.H., Kim, E.-J., Pan, J.-G., Kwon, O., Oh, G.T., 2020. SOD1 suppresses pro-inflammatory immune responses by protecting against oxidative stress in colitis. Redox Biol 37, 101760. https://doi.org/10.1016/j.redox.2020.101760

Kimball, A.L., McCue, P.M., Petrie, M.A., Shields, R.K., 2018. Whole body heat exposure modulates acute glucose metabolism. International Journal of Hyperthermia 35, 644–651. https://doi.org/10.1080/02656736.2018.1516303

Kisliouk, T., Cramer, T., Meiri, N., 2017. Methyl CpG level at distal part of heat-shock protein promoter HSP70 exhibits epigenetic memory for heat stress by modulating recruitment of POU2F1-associated nucleosome-remodeling deacetylase (NuRD) complex. Journal of Neurochemistry 141, 358–372. https://doi.org/10.1111/jnc.14014

Koepsell, H., 2020. Glucose transporters in the small intestine in health and disease. Pflugers Arch 472, 1207–1248. https://doi.org/10.1007/s00424-020-02439-5

Lee, M.-C., Velayutham, M., Komatsu, T., Hille, R., Zweier, J.L., 2014. Measurement and Characterization of Superoxide Generation from Xanthine Dehydrogenase: A Redox-Regulated Pathway of Radical Generation in Ischemic Tissues. Biochemistry 53, 6615–6623. https://doi.org/10.1021/bi500582r

Li, H., Wu, Q., Xu, L., Li, X., Duan, J., Zhan, J., Feng, J., Sun, X., Chen, H., 2015. Increased oxidative stress and disrupted small intestinal tight junctions in cigarette smoke-exposed rats. Molecular Medicine Reports 11, 4639–4644. https://doi.org/10.3892/mmr.2015.3234

Liang, Q., Huan, S., Lin, Y., Su, Z., Yao, X., Li, C., Ji, Z., Zhang, X., 2024. Screening of heat stress-related biomarkers in chicken serum through label-free quantitative proteomics. Poultry Science 103, 103340. https://doi.org/10.1016/j.psj.2023.103340

Liemburg-Apers, D.C., Willems, P.H.G.M., Koopman, W.J.H., Grefte, S., 2015. Interactions between mitochondrial reactive oxygen species and cellular glucose metabolism. Arch Toxicol 89, 1209–1226. https://doi.org/10.1007/s00204-015-1520-y

Liu, H., Dicksved, J., Lundh, T., Lindberg, J.E., 2014. Heat Shock Proteins: Intestinal Gatekeepers that Are Influenced by Dietary Components and the Gut Microbiota. Pathogens 3, 187–210. https://doi.org/10.3390/pathogens3010187

Marchesi, J.A.P., Ibelli, A.M.G., Peixoto, J.O., Cantão, M.E., Pandolfi, J.R.C., Marciano, C.M.M., Zanella, R., Settles, M.L., Coutinho, L.L., Ledur, M.C., 2019. Whole transcriptome analysis of the pectoralis major muscle reveals molecular mechanisms involved with white striping in broiler chickens. Poultry Science 98, 590–601. https://doi.org/10.3382/ps/pey429

Marchewka, J., Sztandarski, P., Zdanowska-Sąsiadek, Ż., Adamek-Urbańska, D., Damaziak, K., Wojciechowski, F., Riber, A.B., Gunnarsson, S., 2021. Gastrointestinal Tract Morphometrics and Content of Commercial and Indigenous Chicken Breeds with Differing Ranging Profiles. Animals 11, 1881. https://doi.org/10.3390/ani11071881

Mayorga, E.J., Ross, J.W., Keating, A.F., Rhoads, R.P., Baumgard, L.H., 2020. Biology of heat stress; the nexus between intestinal hyperpermeability and swine reproduction. Theriogenology 154, 73–83. https://doi.org/10.1016/j.theriogenology.2020.05.023

692 Mu, Q., Kirby, J., Reilly, C.M., Luo, X.M., 2017. Leaky Gut As a Danger Signal for
693 Autoimmune Diseases. Frontiers in Immunology 8.
694 https://doi.org/10.3389/fimmu.2017.00598
695 Nakrani, M.N., Wineland, R.H., Anjum, F., 2024. Physiology, Glucose Metabolism, in:
696 StatPearls. StatPearls Publishing, Treasure Island (FL).
697 Paital, B., Panda, S.K., Hati, A.K., Mohanty, B., Mohapatra, M.K., Kanungo, S., Chainy,
698 G.B.N., 2016. Longevity of animals under reactive oxygen species stress and disease
699 susceptibility due to global warming. World J Biol Chem 7, 110–127.
700 https://doi.org/10.4331/wjbc.v7.i1.110
701 Pei, J., Pan, X., Wei, G., Hua, Y., 2023. Research progress of glutathione peroxidase family
702 (GPX) in redoxidation. Front Pharmacol 14, 1147414.
703 https://doi.org/10.3389/fphar.2023.1147414
704 Rashid, A., Sharma, S.K., Tyagi, J.S., Mohan, J., Narayan, R., Kolluri, G., Singh, R.P., n.d.
705 Incubation Temperatures Affect Expression of Nutrient Transporter Genes in Japanese
706 Quail. Asian Journal of Animal and Veterinary Advances 11, 538–547.
707 https://doi.org/10.3923/ajava.2016.538.547
708 Rhoads, R.P., Baumgard, L.H., Suagee, J.K., Sanders, S.R., 2013. Nutritional Interventions to
709 Alleviate the Negative Consequences of Heat Stress. Advances in Nutrition 4, 267–276.
710 https://doi.org/10.3945/an.112.003376
711 Rosenberg, T., Kisliouk, T., Ben-Nun, O., Cramer, T., Meiri, N., n.d. Cross-tolerance: embryonic
712 heat conditioning induces inflammatory resilience by affecting different layers of epigenetic
713 mechanisms regulating IL6 expression later in life. Epigenetics 16, 228–241.
714 https://doi.org/10.1080/15592294.2020.1795596
715 Rosenberg, T., Marco, A., Kisliouk, T., Haron, A., Shinder, D., Druyan, S., Meiri, N., 2022.
716 Embryonic heat conditioning in chicks induces transgenerational heat/immunological
717 resilience via methylation on regulatory elements. The FASEB Journal 36, e22406.
718 https://doi.org/10.1096/fj.202101948R
719 Rostagno, M.H., 2020. Effects of heat stress on the gut health of poultry. J Anim Sci 98,
720 skaa090. https://doi.org/10.1093/jas/skaa090
721 Shandilya, S., Kumar, S., Kumar Jha, N., Kumar Kesari, K., Ruokolainen, J., 2022. Interplay of
722 gut microbiota and oxidative stress: Perspective on neurodegeneration and neuroprotection.
723 Journal of Advanced Research 38, 223–244. https://doi.org/10.1016/j.jare.2021.09.005
724 Siddiqui, S.H., Kang, D., Park, J., Khan, M., Shim, K., 2020. Chronic heat stress regulates the
725 relation between heat shock protein and immunity in broiler small intestine. Sci Rep 10,
726 18872. https://doi.org/10.1038/s41598-020-75885-x
727 Sun, B., Chen, H., Xue, J., Li, P., Fu, X., 2023. The role of GLUT2 in glucose metabolism in
728 multiple organs and tissues. Mol Biol Rep 50, 6963–6974. https://doi.org/10.1007/s11033-
729 023-08535-w
730 Sun, X., Zhang, H., Sheikhahmadi, A., Wang, Y., Jiao, H., Lin, H., Song, Z., 2015. Effects of
731 heat stress on the gene expression of nutrient transporters in the jejunum of broiler chickens
732 (Gallus gallus domesticus). Int J Biometeorol 59, 127–135. https://doi.org/10.1007/s00484-
733 014-0829-1
734 Wang, Y.-C., Leng, X.-X., Zhou, C.-B., Lu, S.-Y., Tsang, C.K., Xu, J., Zhang, M.-M., Chen, H.-
735 M., Fang, J.-Y., 2022. Non-enzymatic role of SOD1 in intestinal stem cell growth. Cell
736 Death Dis 13, 1–13. https://doi.org/10.1038/s41419-022-05267-w

737 Watford, M., 1985. Gluconeogenesis in the chicken: regulation of phosphoenolpyruvate
738 carboxykinase gene expression. Fed Proc 44, 2469–2474.
739 Yoshikawa, T., Inoue, R., Matsumoto, M., Yajima, T., Ushida, K., Iwanaga, T., 2011.
740 Comparative expression of hexose transporters (SGLT1, GLUT1, GLUT2 and GLUT5)
741 throughout the mouse gastrointestinal tract. Histochem Cell Biol 135, 183–194.
742 https://doi.org/10.1007/s00418-011-0779-1
743 Zhang, C., Zhao, X.H., Yang, L., Chen, X.Y., Jiang, R.S., Jin, S.H., Geng, Z.Y., 2017.
744 Resveratrol alleviates heat stress-induced impairment of intestinal morphology, microflora,
745 and barrier integrity in broilers. Poultry Science 96, 4325–4332.
746 https://doi.org/10.3382/ps/pex266